Comparison of the Chemical Properties of Iron and Cobalt Porphyrins and Corrins

Kasper P. Jensen and Ulf Ryde*[a]

Density functional calculations have been used to compare various geometric, electronic and functional properties of iron and cobalt porphyrin (Por) and corrin (Cor) species. The investigation is focussed on octahedral $M^{II/III}$ complexes (where M is the metal) with two axial imidazole ligands (as a model of b *and* c *type cytochromes) or with one imidazole and one methyl ligand (as a model of methylcobalamin). However, we have also studied some five-coordinate M^{II} complexes with an imidazole ligand and four-coordinate $M^{I/II}$ complexes without any axial ligands as models of other intermediates in the reaction cycle of coenzyme B_{12}. The central cavity of the corrin ring is smaller than that of porphine. We show that the cavity of corrin is close to ideal for low-spin Co^{III}, Co^{II}, and Co^{I} with the axial ligands encountered in biology, whereas the cavity in porphine is better suited for intermediate-spin states. Therefore, the low-spin state of Co is strongly favoured in complexes with corrins, whereas there is a small energy difference between the various spin states in iron porphyrin species. There are no clear differences for the reduction potentials of the octahedral complexes, but $[Co^{I}Cor]$ is more easily formed (by at least 40 kJ $mole^{-1}$) than $[Fe^{I}Por]$. Cobalt and corrin form a strong Co–C bond that is more stable against hydrolysis than iron and porphine. Finally, $Fe^{II/III}$ gives a much lower reorganisation energy than $Co^{II/III}$; this is owing to the occupied d_{z^2} orbital in Co^{II}. Altogether, these results give some clues about how nature has chosen the tetrapyrrole rings and their central metal ion.*

KEYWORDS:

cobalamin · density functional calculations · haem · iron · porphyrin

Introduction

Two of the most remarkable chemical entities of living matter are the porphine and corrin rings. These two systems are vital for a tremendous amount of biochemical reactions, which range from oxygen transport, electron transfer and oxidative metabolism in the case of porphyrin,[1] to alkyl migration and methylation reactions in the case of corrin.[2–4] In spite of their differing functions, their structures are quite similar. The porphine ring has D_{4h} symmetry, with four pyrrole rings connected by methine bridges. As can be seen in Figure 1, the only two things that distinguish the two ring systems are the absence of one of the four methine bridges in corrin, a feature that lowers symmetry to C_{2v}, and ten saturated carbon atoms at the periphery of the corrin ring, which destroys the conjugation of the outer part of the ring and lowers the symmetry to C_1.

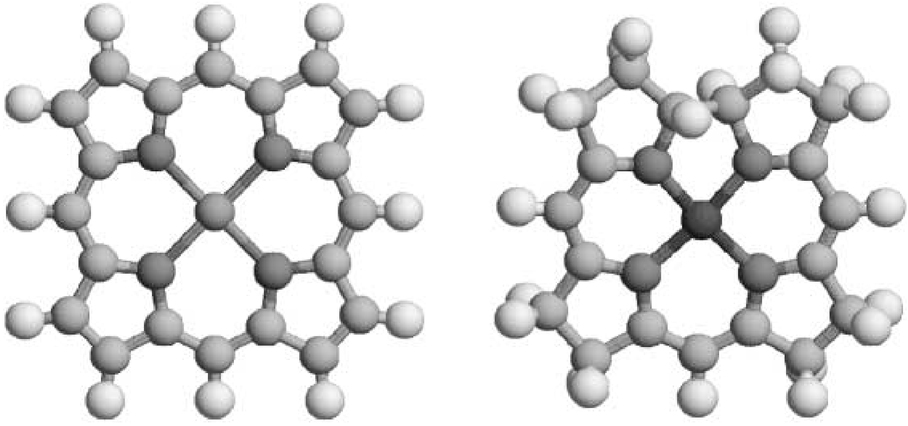

Figure 1. *The porphyrin (left) and corrin (right) ring systems.*

Nature seems to have a clear preference for iron as the central metal ion in porphyrin cofactors, whereas cobalt is normally found only in corrins. Among the first-row transition metals, cobalt has the lowest abundance in sea water together with scandium,[5] but still it is present in the ubiquitous coenzyme B_{12}. Cobalt resides between iron and nickel in the first row of the d block. It has common oxidation states of +II and +III, as does iron, but cobalt may even be reduced to a formal oxidation number of +I in vivo, a property that iron does not possess.[6] On the other hand, iron porphyrin complexes are well-known for their accessible high-valency states (formally Fe^{IV} and Fe^{V}), which play an important role in the function of haem oxidases.[7]

The corrins exist in nature in the form of cobalamins. The B_{12} coenzymes contain a corrin ring with a d^6 low-spin Co^{III} ion in their octahedral resting states. In most cobalamin-dependent enzymes, the imidazole side chain of a histidine residue

---

[a] Dr. U. Ryde, K. P. Jensen
Department of Theoretical Chemistry
Lund University, Chemical Centre
P.O. Box 124, 22100 Lund (Sweden)
Fax: (+46) 46 2224543
E-mail: Ulf.Ryde@teokem.lu.se

DOI: 10.1002/cbic.200200449

coordinates to the cobalt ion. In another group of enzymes, cobalt binds to the pendant dimethylbenzimidazole group of the coenzyme, the properties of which is quite similar to those of an imidazole ligand.[8] The second axial site is occupied by a methyl or 5′-deoxyadenosyl group; these form an organometallic Co–C bond. This bond is broken during the catalytic cycle to form either a five-coordinate Co^{II} intermediate and an adenosyl radical, or a four-coordinate Co^{I} ion, where the imidazole ligand has dissociated and the methyl group has been transferred to a nucleophilic substrate.[2, 9]

Haem enzymes show a larger variation in their axial ligands (His, Cys, Met, Tyr, Glu, Asp, amino terminal, or exogenous ligands), depending on the function.[9] The haem group can be either five-coordinate with an open coordination site where a substrate binds, or six-coordinate with one or two ligands from the protein. However, the most common ligand is a histidine imidazole group, as is present, for example, in myoglobin, haemoglobin, peroxidases, haem oxygenase and most types of cytochromes.[10]

The aim of this paper is to study how the chemical properties of cobalt and iron, as well as porphyrin and corrin, differ. In particular, we want to understand why cobalt is associated with corrins and iron with porphyrins in nature. We have concentrated our study on one typical reaction for each of the two coenzymes, namely, the breakage of the Co–C bond as a typical reaction example of coenzyme B_{12} metabolism, and electron transfer as a typical reaction example for the haem-containing cytochromes.

Several authors have addressed similar questions.[11–19] It has been suggested that corrin was selected to fit the smaller Co^{III} ion.[11, 13, 19] Williams has proposed that low-spin Co^{II} is unique among the available first-row transition metal ions to provide a stable and directed one-electron radical.[17] On the other hand, Pratt has attributed the choice of cobalt to the low 3d to 4s/4p promotion energy of Co^{II}, which gives strong Co–C bonds, because the 3d orbitals are too small to form strong covalent bonds with carbon.[11, 19] Moreover, he argues that corrin was chosen because it forms dimers with an appropriate Co–Co distance. Others have emphasised the flexibility of the corrin ring as an important factor in the labilisation of the Co–C bond.[14, 15] Specifically, the mechanochemical trigger mechanism has been a major argument in favour of a specialised function of corrin systems, based on release of strain energy during catalysis. However, recent experimental[20–22] and theoretical[23, 24] results have indicated that such a conformational change is unlikely to drive a catalytic reaction within corrins. Finally, Rovira et al. have compared the geometric and electronic structure of four-coordinate cobalt complexes with corrin and porphine by using theoretical calculations.[16] They show that the excitation energy associated with $d_{x^2-y^2}$ occupation is much higher in corrins than in porphyrins.

Our investigation is based on similar density functional calculations. During recent years, such methods have successfully been applied to the study of both iron porphyrin species[25–37] and coenzyme B_{12} models.[16, 24, 38–42] Theoretical methods have the advantage of being cheap and fast while giving 'pure' results (well-defined reactions in vacuum). On the other hand, solvation effects and free energies are hard to describe in a consistent way, and the accuracy is limited. In this paper, we study how the geometry, thermodynamic stability, spin energies, electronic structure, reduction potential, reorganisation energy and Co–C bond dissociation energy differ for iron and cobalt porphyrin and corrin species. The results are discussed in relation to the earlier suggestions.

Results and Discussion

Spin-splitting energies

Several authors have suggested that porphine and corrin ligands were selected to make low-spin (LS) states available for iron and cobalt, because the natural amino acid ligands provide too weak a ligand field to drive iron or cobalt ions into the LS state.[13, 17, 43] This is probably most important for Co^{II}, for which the vast majority of ligands give rise to a high-spin (HS) state.[13] Moreover, it has been suggested that porphyrin was selected to keep iron centres close to the crossover point between the LS, intermediate-spin (IS) and HS states.[17]

In order to check these suggestions and to compare the relative strength of the porphine and corrin ligand fields and the intrinsic preferences of iron and cobalt, we have studied the energy differences between the LS, IS and HS states of the octahedral imidazole/methyl (Im/Me) complexes (both M^{II} and M^{III}) and the square-pyramidal Im complexes (only M^{II}), with all four combinations of Fe/Co and Por/Cor. All structures were fully geometry optimised. It should be noted that the calculated spin-splitting energies are appreciably less accurate than other estimates in this paper because they are calculated as differences between different spin states, which means that errors in the correlation energy are less likely to cancel out. Yet, *differences* in spin-splitting energies between Fe and Co or Por and Cor should be reliable.

Unfortunately, it turned out that only one octahedral Im/Me complex was stable in the HS state, [Fe^{II}PorImMe]. All the other complexes lost the imidazole ligand during the optimisation. The same applies also to the IS [Co^{II}CorImMe] complex. (Note that Co^{II} has seven d electrons and therefore does not have a sextet state comparable to the HS quintet state of Fe^{II}.) Therefore, only the energy difference between the LS and IS states is presented in Table 1.

For these octahedral Im/Me complexes, all combinations of metals and ring systems give rise to an LS ground state, in accordance with experimental results for cobalt corrin species.[44] The IS states are 46–139 kJ mole^{-1} higher in energy for the M^{III} complexes. The difference is ≈40 kJ mole^{-1} larger for Co than for

Table 1. The energy difference [kJ mol^{-1}] between the low-spin and intermediate-spin states of the [MCor/PorImMe] complexes.

	Fe^{II}	Co^{II}	Fe^{III}	Co^{III}
porphyrin	39	78	46	82
corrin	35	–[a]	92	139

[a] No stable octahedral minimum for the quartet state.

Fe and also ≈50 kJ mol^{-1} larger for Cor than for Por. The difference is slightly smaller for the M^{II} complexes, with a similar difference between Co and Fe. Thus, our calculations confirm that both Cor and Por give rise to strong ligand fields and that Fe and Por give complexes quite close to the spin-crossover point.

The spin-splitting energies of the five-coordinate Im complexes are even more interesting, because for these we expect to find a difference in the preferred ground state. Experimentally, cob(II)alamin is LS whereas five-coordinate Fe^{II} haem is normally HS, for example, in deoxymyoglobin.[7] The results in Table 2 partly confirm this observation: The two cobalt complexes have LS ground states, with an energy difference of 21 (porphine) and 58 kJ mol^{-1} (corrin) to the IS states. However, for [Fe^{II}PorIm] the calculations indicate that IS is actually 4 kJ mol^{-1} more stable than the HS state. This amount of energy is so small that it may be caused by deficiencies in the method or by the neglect of environmental effects. Similar results have been obtained in earlier calculations.[35] Clearly, the results confirm the shift of the ground state from LS.

Table 2. *The energy difference [kJ mol^{-1}] between the various spin states of the five-coordinate [M^{II}Cor/PorIm] complexes and the four-coordinate [M^{I}Cor/Por] complexes.*

Spin state	LS	IS	HS
[Fe^{II}PorIm]	28	0	4
[Fe^{II}CorIm]	21	0	29
[Co^{II}PorIm]	0	21	
[Co^{II}CorIm]	0	58	
[Fe^{I}Por]	0	13	28
[Fe^{I}Cor]	0	31	112
[Co^{I}Por]	0 (−18[a])	4	
[Co^{I}Cor]	0 (−4[a])	75	

[a] Open-shell singlet state.

Similar results are also obtained for the four-coordinate M^{I} complexes. All these are most stable in the LS state. However, for the iron porphine complexes, the IS and sometimes also the HS states are low-lying. Interestingly, the cobalt complexes are most stable in the open-shell singlet state, formed by antiferromagnetical coupling between Co^{II} and a ring radical. This has not been observed before,[16] but for Co^{I}Cor the energy difference to the closed-shell LS state is only 4 kJ mol^{-1}, that is, within the uncertainty of the method.

In conclusion, the spin-splitting energies indicate that cobalt and corrin favour the LS state, whereas Fe and Por give a small splitting between the various states. In the rest of this article we will study only model complexes in their electronic ground states.

Thermodynamic stability

Considering the in vivo abundance of iron porphyrins and cobalt corrins, it is natural to address the relative thermodynamic stability of these complexes. Stability considerations may explain why iron forms biological complexes with porphyrin rather than corrin and why the opposite is the case for cobalt. With theoretical means, we can calculate the reaction energy of the hypothetical isodesmic reaction from Equation (1), where X represents various sets of axial ligands and all metals are in the same oxidation state, M^{I}, M^{II} or M^{III}.

$$\mathrm{CoCor}X + \mathrm{FePor}X \rightarrow \mathrm{CoPor}X + \mathrm{FeCor}X \qquad (1)$$

This reaction energy quantifies the change in energy obtained by replacing Co in the corrin ring with Fe from the porphine, and vice versa. The energy obtained for this reaction with various axial ligands and oxidation states of the metals is shown in Table 3. It can be seen that the reaction energies are quite small (8–22 kJ mol^{-1}) as are the solvation effects, 0–4 kJ mol^{-1}. In all except one case, the reaction energies are positive; this indicates that the native combination of ions and ring systems is more stable than the alternative. However, for the Im/Me complexes with M^{II} ions, the reaction energy is negative, which indicates that the nonnative combination is more stable. This may be an effect of the differing electronic states for Co^{II} in these complexes (see below).

Table 3. *Thermodynamic stabilities [Eq. (1)] of complexes with various axial ligands and oxidation states, calculated at different values of the dielectric constant (ε).*

Axial ligands	Oxidation state	$\varepsilon = 1$	$\varepsilon = 4$	$\varepsilon = 80$
Im$_2$	+II	12.2	10.7	9.6
	+III	7.8	8.0	8.1
Im/Me	+II	−13.2	−12.5	−11.4
	+III	16.8	17.0	17.1
Im/OH	+III	18.6	15.9	14.1
Im	+II	14.2	14.3	14.4
–	+I	19.5	20.8	21.1
–	+II	21.4	22.6	23.9

These energies include all chemical differences between the two ions and the two ring systems, for example, ionic radii, chemical softness and effective charge. However, they do not give any indication about which of these properties may be important for the selection. Moreover, we expect that besides these thermodynamic preferences, there should also be some *functional* reason for the selection of ions and ring systems. This will be investigated in the forthcoming sections.

Geometries and the size of the ring cavities

Next, we examine the geometries of the various complexes. In particular, we will discuss the size of the central cavities of the ring systems and compare them to the size of the ions, because it has been suggested that Cor was selected because of its smaller cavity, which would fit Co^{III} properly.[11, 13, 19, 45] The geometries of the optimised FePor and CoCor species are shown in Figure 2 (the corresponding CoPor and FeCor complexes are closely similar).

The metal–ligand distances of the optimised Im/Me and Im$_2$ models are collected in Tables 4 and 5, respectively. The M–C

Table 4. *Metal – ligand bond distances [pm] of the optimised [MCor/PorImMe] complexes in their low-spin ground states.*

Structure	M–C	M–N$_{\mathrm{Im}}$	M–N$_{\mathrm{eq,av}}$
$[\mathrm{Fe^{II}PorImMe}]^-$	200.5	222.8	201.5
$[\mathrm{Fe^{II}CorImMe}]^0$	201.0	226.0	192.1
$[\mathrm{Co^{II}PorImMe}]^{-1}$	195.2	220.4	202.0
$[\mathrm{Co^{II}CorImMe}]^0$	195.9	225.2	192.8
$[\mathrm{Fe^{III}PorImMe}]^0$	198.9	224.9	201.8
$[\mathrm{Fe^{III}CorImMe}]^+$	199.6	229.0	193.3
$[\mathrm{Co^{III}PorImMe}]^0$	195.7	221.2	200.6
$[\mathrm{Co^{III}CorImMe}]^+$	196.6	225.0	192.0

Table 5. *Metal – ligand bond distances [pm] of the optimised [MCor/PorIm$_2$] complexes in their low-spin ground states.*

Structure	M–N$_{\mathrm{Im1}}$	M–N$_{\mathrm{Im2}}$	M–N$_{\mathrm{eq,av}}$
$[\mathrm{Fe^{II}PorIm_2}]^-$	202.4	204.5	204.5
$[\mathrm{Fe^{II}CorIm_2}]^0$	206.0	209.1	193.5
$[\mathrm{Co^{II}PorIm_2}]^{-1}$	240.0	240.1	201.2
$[\mathrm{Co^{II}CorIm_2}]^0$	247.3	251.0	192.1
$[\mathrm{Fe^{III}PorIm_2}]^0$	201.2	202.6	202.6
$[\mathrm{Fe^{III}CorIm_2}]^+$	204.7	204.8	193.5
$[\mathrm{Co^{III}PorIm_2}]^0$	197.9	198.1	200.6
$[\mathrm{Co^{III}CorIm_2}]^+$	199.5	201.6	192.5

bond lengths are longer for iron (199 – 201 pm) than for the cobalt complexes (195 – 197 pm), but there is no significant difference between the Cor and Por rings.

The M–N$_{\mathrm{Im}}$ distances vary more, which reflects the fact that this bond is weaker and more flexible.[24] For the Im/Me complexes, the M–N$_{\mathrm{Im}}$ bonds are rather long, 217 – 229 pm. They are longer for Fe than for Co and longer for Por than for Cor. For the Im$_2$ complexes, the two M–N$_{\mathrm{Im}}$ distances are quite similar in length and shorter (198 – 209 pm) than in the Im/Me complexes. This is, of course, caused by the negative charge of the methyl ligand, which elongates the bonds of the other ligands, especially for the flexible Im ligand. However, in the Co$^{\mathrm{II}}$ complexes, the M–N$_{\mathrm{Im}}$ bonds are very long (240 – 251 pm). The reason for this is that low-spin Co$^{\mathrm{II}}$ is a d^7 ion, with an electron in the d$_{z^2}$ orbital, which is directed towards the axial ligands, thereby destabilising these interactions.

However, the most systematic differences are found for the equatorial M–N$_{\mathrm{eq}}$ distances: Porphine always has M–N$_{\mathrm{eq}}$ bonds that are ≈9 pm longer

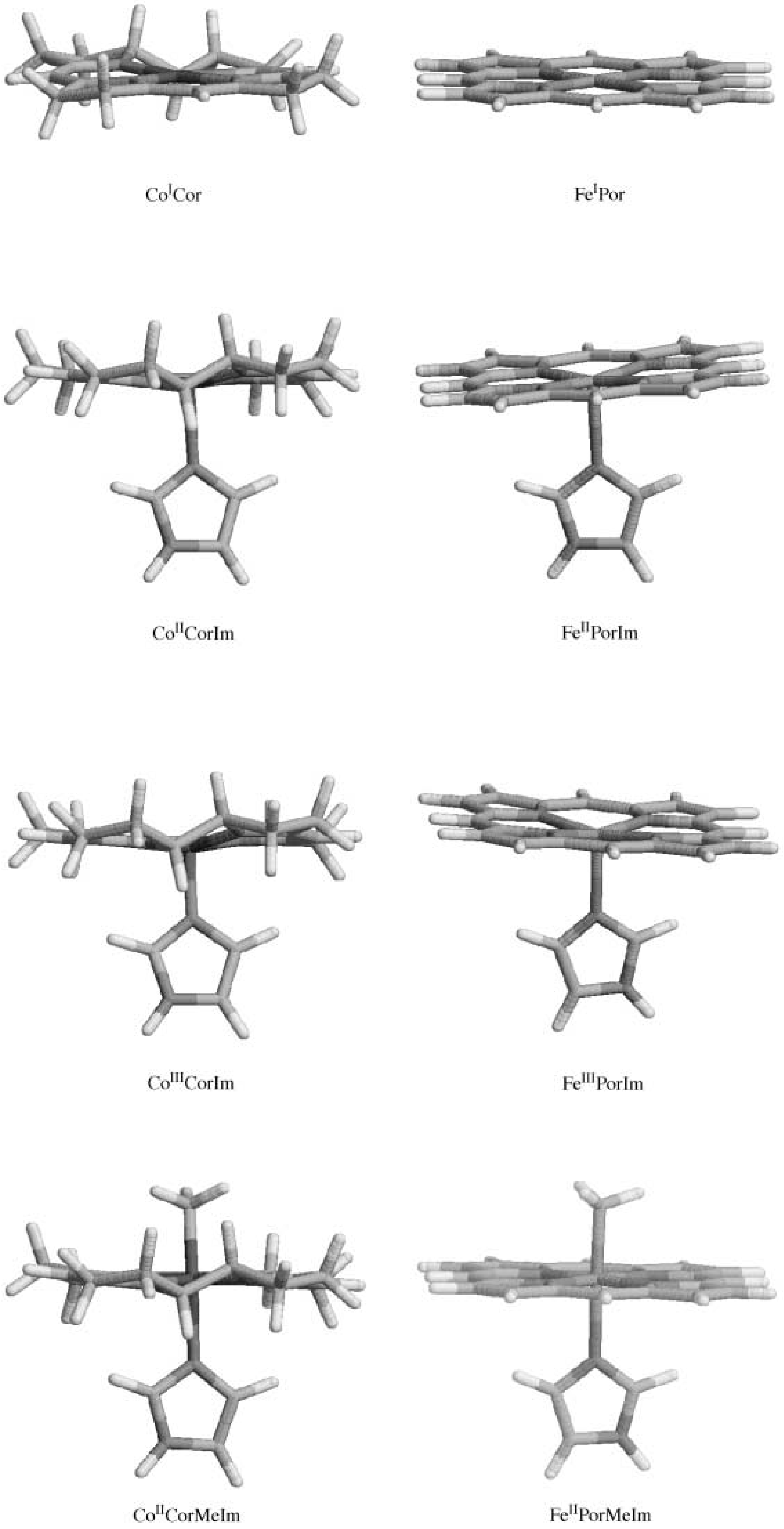

Figure 2. *Optimised structures of the studied cobalt corrin and iron porphyrin complexes.*

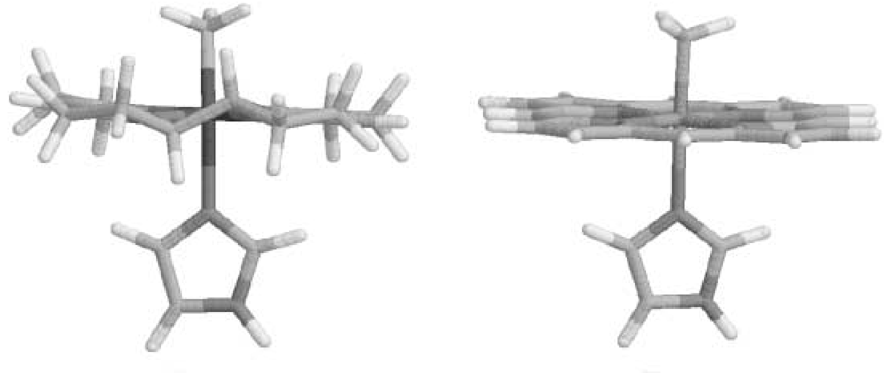

Co^{III}CorMeIm

Fe^{III}PorMeIm

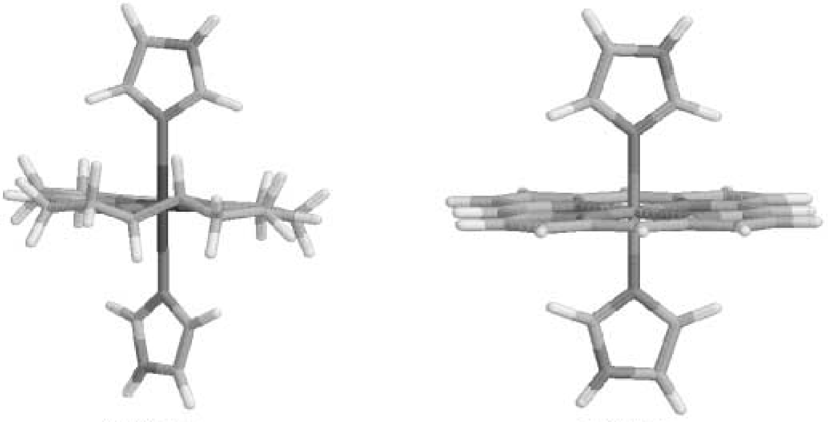

Co^{II}CorIm$_2$

Fe^{II}PorIm$_2$

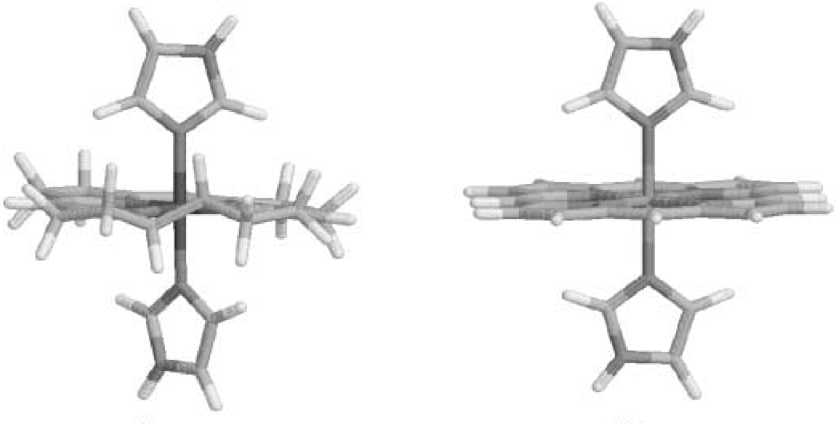

Co^{III}CorIm$_2$

Fe^{III}PorIm$_2$

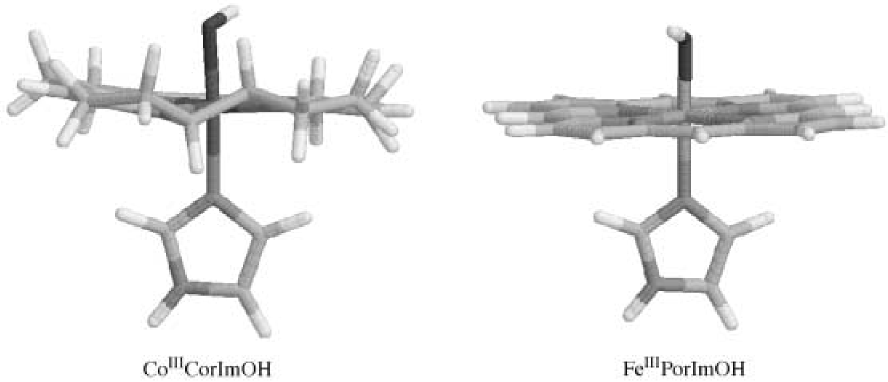

Co^{III}CorImOH

Fe^{III}PorImOH

Figure 2. *(Continued)*

(201 – 207 pm) than corrin (192 – 193 pm). On the other hand, these bonds show no clear trends with respect to the metal ion or oxidation states. This indicates that the M–N$_{eq}$ distances are mainly determined by the inherent size of the central cavity of the rings and can only barely be modified by the metal.

To test this, we calculated the *trans* N$_{eq}$–N$_{eq}$ distance in free dianionic porphine. It is 417 pm after geometry optimisation. The corresponding distance in free anionic corrin is 395 pm (on average; the ring is distinctly nonplanar with *trans* N$_{eq}$–N$_{eq}$ distances of 377 pm and 413 pm). Thus, the cavity is 22 pm smaller in corrin than in porphyrin, owing to the missing methine bridge; this is in good accordance with the 9 pm difference found for the M–N$_{eq}$ bonds.

Thus, the differing cavity size can be an important factor in the selection of ions for the two ring systems. However, this alone cannot explain why cobalt is found in corrins and iron in porphyrins. On the contrary, the ionic radii for low-spin octahedral Fe^{III} and Co^{III} are equal (55 pm), whereas the ionic radius of Co^{II} (65 pm) is actually slightly *larger* than that of Fe^{II} (61 pm).[44] Instead, it seems likely that the porphyrin ring was selected to allow spin states other than low spin; high-spin octahedral Fe^{II} and Fe^{III} have ionic radii of 78 and 65 pm, respectively.[44]

In order to test such a suggestion, we need to know the ideal bond length of iron and cobalt in porphyrin and corrin models with the particular ligands of interest. This can be studied by cutting the ring into two $NH(CH)_3NH^-$ moieties, as has been done before.[36] From Figure 3, it can be seen that such a model retains the number of carbon atoms in the chelate ring and the hybridisation of the ring systems, but it removes any restraints imposed by the ring system. Moreover, the same model is appropriate for both porphyrin and corrin, except for the additional charge in porphyrin compared to corrin. Therefore, the optimum M–N$_{Im}$ distances in models with this ligand can be expected to reflect the ideal bond length of that metal with the same axial ligands in a tetrapyrrole ring system.

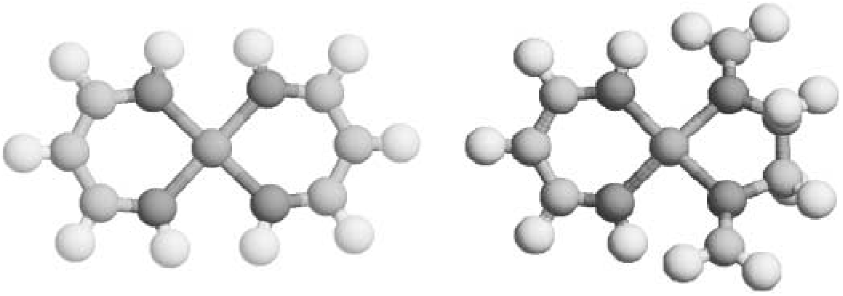

Figure 3. The [M(NH(CH)$_3$NH)$_2$] (left) and [M(NH(CH)$_3$NH)(NCH$_2$(CH$_2$)$_2$NCH$_2$)] (right) models with removed ring strain.

We have optimised the structure of [M(NH(CH)$_3$NH)$_2$Im$_2$] with Co and Fe in both oxidation states. The results in Table 6 clearly illustrate the rigidity of the porphyrin and corrin rings. When the rings are broken, the M—N$_{eq}$ distances change significantly. The Fe^{II}—N$_{eq}$ distance is 199 pm, which is 4 pm longer than in corrin and and 6 pm shorter than in porphyrin. The Fe^{III}—N$_{eq}$ bonds are 194 pm long, which is close to the bond lengths found in corrin, but 9 pm shorter than in porphyrin. The difference between Fe^{II} and Fe^{III} (5 pm) is close to the difference in ionic radii of the two ions (6 pm), which shows that the calculations are reliable.

Table 6. Calculated metal – ligand distances [pm] for four types of complexes with the ligand L = (NH(CH)$_3$NH), which simulates a broken ring system. The M—N$_{eq}$ distances for the corresponding porphyrin and corrin complexes are also included for comparison.

Structure	M—N$_{Im1}$	M—N$_{Im2}$	M—N$_{eq,av}$	Cor	Por
[Fe^{II}L$_2$Im$_2$]	205.4	205.4	198.8	193.5	204.5
[Fe^{III}L$_2$Im$_2$]	204.7	204.7	194.0	193.5	202.6
[Co^{II}L$_2$Im$_2$]	250.4	254.6	194.5	192.1	201.2
[Co^{III}L$_2$Im$_2$]	199.3	199.3	193.9	192.5	200.6
[Co^{III}L$_2$ImMe]	227.4	195.7	193.6	192.0	200.6
[Co^{II}L$_2$Im]	228.5	–	195.3	192.1	200.6
[Co^{I}L$_2$]	–	–	190.4	188.6	198.8

The Co^{III}—N$_{eq}$ distance is the same as for Fe^{III} (194 pm), in excellent agreement with their identical ionic radii. However, in porphyrin and corrin, Co^{III} gives bonds that are 1 – 2 pm shorter than those of Fe^{III}, which indicates that Co^{III} forms stronger (more covalent) bonds than Fe^{III}. The Co^{II}—N$_{eq}$ bonds in [Co(NH(CH)$_3$NH)$_2$Im$_2$] are 7 pm shorter than in porphyrin and 2 pm longer than in corrin.

Altogether, these results show that porphyrin and corrin form rather rigid ring systems that allow for only small variations in the M—N$_{eq}$ bond lengths. Interestingly, porphyrin with its double charge seems to be more flexible (201 – 207 pm) than the monoanionic corrin ring (192 – 194 pm). The central cavity of porphyrin is appreciably larger (6 – 9 pm) than the ideal bond length of all ions considered in this investigation. This indicates that the cavity would be ideal for ions with a radius of 62 – 67 pm (similar results have been obtained with other methods).[45] Thus, it would be ideal for the HS (65 pm) and IS states of Fe^{III} and close to ideal for HS Co^{III} (61 pm)[44] On the other hand, it is still too small for the (octahedral) HS states of Fe^{II} (78 pm) and Co^{II} (75 pm). This lends support to the suggestion that porphyrin was selected to allow various spin states of iron.

The central cavity of corrin is appreciably smaller than that of porphyrin. It is close to the ideal bond length of the LS state of all ions in this investigation (within 2 pm), except Fe^{II}, for which it is 5 pm too small. Thus, it is proper for ions with a radius of 54 – 56 pm. This means that all ions in the HS state are too large to fit properly into the cavity. Hence, the corrin ring, in contrast to porphyrin, selectively stabilises the LS states of the ions. Moreover, it fits excellently both Co^{II} and Co^{III}, but not Fe^{II}. Thus, corrin seems to be an ideal ligand for LS cobalt chemistry. This is most likely a strong reason why corrin is selected for cobalt chemistry, whereas porphyrin is employed in iron chemistry.

To see if the cavity size of corrin is also appropriate for the actual intermediates in the reaction cycles of coenzyme B$_{12}$, we have compared the Co—N$_{eq}$ bond lengths of [Co^{III}CorImMe], [Co^{II}CorIm] and [Co^{I}Cor] (LS states) with the corresponding complexes with the broken-ring ligand NH(CH)$_3$NH. The results are also included in Table 6 and they show that the Co—N$_{eq}$ distance increases by 2 – 3 pm when the corrin ring is broken in all three complexes. Therefore, we can conclude that the corrin ligand is close to optimal (within 3 pm) for all relevant oxidation states and ligands of LS cobalt, especially as the method B3LYP normally overestimates metal – ligand bond lengths by a few pm.[38]

We have also tested an alternative ring-broken model, applicable for the corrin ring (with the correct single negative charge), [M(NH(CH)$_3$NH)(NCH$_2$(CH$_2$)$_2$NCH$_2$)] (see Figure 3). However, it turned out that this ligand was too crowded so that the two ring fragments do not always stay in the same plane and that the individual M—N$_{ax}$ bond lengths differ strongly, for example, two bonds of 190 pm and two of 206 – 208 pm for the [Fe^{III}Im$_2$] complex (for the NH(CH)$_3$NH ligand, the individual bond lengths vary by less than 0.4 pm). Therefore, these results were judged to be less reliable, although they give a similar average M—N$_{ax}$ bond length to NH(CH)$_3$NH for most of the complexes.

Finally, we note that the present results also provide a qualitative explanation of the spin-splitting energies discussed above (see Tables 1 and 2). Corrin is more rigid than porphyrin and has a cavity size close to the ionic radius of the low-spin states of all ions, except Fe^{II}. Therefore, the spin-splitting energies are appreciably larger for corrin than for porphyrin for all complexes, except Fe^{II}.

Interestingly, porphyrin ruffling has been invoked to explain how various metal ions may shorten the otherwise unfavourable, long Co—N bonds,[46] which result from the large cavity size of porphyrin.[47] However, as opposed to the ruffled ground state observed for sterically crowded nickel porphyrin species,[59] all the porphyrin complexes investigated here are completely planar, regardless of spin state, as can be seen for the FePor complexes in Figure 2. Thus, the differing cavity sizes of corrin and porphyrin are basic features of the planar systems.

Figure 2 also shows the structures of all the optimised CoCor complexes. These complexes are distinctly nonplanar, as an effect of the missing methine linkage and the saturated atoms in the ring system. The distortion of the corrin ring is normally measured as the fold angle, defined as the angle between the two average planes formed by the seven inner atoms in the corrin ring on both sides of a line from the missing methine link to the opposite methine atom.[2] It is 4 – 7° (lowest for the Im/Me complexes and largest for the Im/OH complexes) in the investigated complexes, without any systematic differences between iron and cobalt.

Electronic structure

In order to compare the electronic structures of the various complexes, we have calculated the Mulliken charges of various groups and atoms. These are collected in Tables 7 and 8 for the Im/Me and Im$_2$ complexes, respectively. They show that the charge on the metal ion (0.54 to 0.85 *e*) and the axial ligands is quite constant (0.1 to 0.3 *e* on imidazole and -0.01 to -0.25 *e* on the methyl group). Consequently, the major difference in the charge density between the various complexes (with a total charge ranging from -1 to $+2$) is found in the ring system: The total charge in the porphyrin ring varies between -1.39 and -0.32 *e* and the corrin charge varies between -0.54 and $+0.64$ *e*.

Table 7. *Mulliken charges, spin density and 3d population on some atoms and groups of atoms in the [MCor/PorImMe] complexes.*

Compound	Charge on					Spin	M 3d
	M	CH$_3$	Im	Ring	4N$_{eq}$	on M	population
[Fe^{II}PorImMe]$^-$	0.57	−0.27	0.08	−1.38	−2.08	–	6.57
[Fe^{II}CorImMe]	0.55	−0.24	0.10	−0.41	−1.78	–	6.62
[Co^{II}PorImMe]$^-$	0.57	−0.09	0.12	−1.60	−2.18	0.00	7.42
[Co^{II}CorImMe]	0.54	−0.08	0.13	−0.59	−1.87	0.01	7.46
[Fe^{III}PorImMe]	0.66	−0.07	0.15	−0.74	−2.19	1.19	6.40
[Fe^{III}CorImMe]$^+$	0.64	−0.05	0.16	0.25	−1.91	1.16	6.44
[Co^{III}PorImMe]	0.56	−0.03	0.16	−0.69	−2.13	–	7.43
[Co^{III}CorImMe]$^+$	0.54	−0.01	0.17	0.30	−1.85	–	7.47

Table 8. *Mulliken charges, spin density and 3d population on some atoms and groups of atoms the [MCor/PorIm$_2$] complexes.*

Compound	Charge on					Spin	M 3d
	M	CH$_3$	Im	Ring	4N$_{eq}$	on M	population
[Fe^{II}PorIm$_2$]	0.67	0.15	0.15	−0.97	−2.08	–	6.54
[Fe^{II}CorIm$_2$]$^+$	0.70	0.17	0.17	−0.04	−1.84	–	6.54
[Co^{II}PorIm$_2$]	0.69	0.12	0.12	−0.92	−2.19	0.99	7.45
[Co^{II}CorIm$_2$]$^+$	0.72	0.13	0.13	0.01	−1.97	1.00	7.45
[Fe^{III}PorIm$_2$]$^+$	0.84	0.26	0.26	−0.36	−2.20	1.07	6.26
[Fe^{III}CorIm$_2$]$^{2+}$	0.85	0.27	0.28	0.60	−1.96	1.02	6.28
[Co^{III}PorIm$_2$]$^+$	0.72	0.30	0.30	−0.32	−2.12	–	7.30
[Co^{III}CorIm$_2$]$^{2+}$	0.73	0.31	0.31	0.64	−1.87	–	7.32

In Tables 7 and 8 we also include the spin density on the metal ion for the various complexes. In all open-shell complexes, the spin density is close to 1 *e*, which indicates that almost all unpaired spin density is located on the metal ion, although there is also a significant spin density on the methyl groups (≈ -0.15 *e*). However, the two Im/Me complexes with Co^{II} differ radically from the other complexes: In these, there is essentially no spin density on Co and Me. Instead, all the spin is found in the porphine or corrin rings. Apparently, it is more favourable in these complexes to form a Por/Cor radical and a Co^{III} ion, which is d^6 with an empty d$_{z^2}$ orbital and therefore forms better bonds with the strong methyl ligand, whereas with the two weaker imidazole ligands the d^7 state is more stable.

Table 9 shows the corresponding results for the four-coordinate M^I/M^{II} complexes with Cor/Por. They are similar to those of the six-coordinate complexes, with a metal charge of 0.50 – 0.74 *e* and a variable ring charge. However, the M^I complexes show some interesting features: The Fe^I complexes are doublets with a spin population close to 2 on Fe (1.9 – 2.0) and with one unpaired electron delocalised in the ring system. Thus, the iron complexes are triplet Fe^{II} species, antiferromagnetically coupled to a porphine or corrin radical. Apparently, the reduction potential of the Fe^{II}/Fe^I couple is lower than the energy needed to form a ring radical. As we saw above, the same is true also for the Co^I complexes: Their lowest electronic states are open-shell singlets, formed from doublet Co^{II}, antiferromagnetically coupled to a ring radical. However, the closed-shell singlets are only 4 – 18 kJ mole^{-1} higher in energy.

Table 9. *Mulliken charges, spin density and 3d population on some atoms and groups of atoms the four-coordinate [MCor/Por] complexes.*

Compound	Charge on			Spin	M 3d
	M	Ring	4N$_{eq}$	on M	population
[Fe^{I}Por]$^-$	0.59	−1.59	−2.37	2.02	6.54
[Fe^{I}Cor]	0.62	−0.62	−2.10	1.94	6.58
[Co^{I}Por]$^-$	0.51	−1.51	−2.33	0.89	7.55
[Co^{I}Por]$^{-[a]}$	0.38	−1.38	−2.24	–	7.72
[Co^{I}Cor]	0.50	−0.50	−2.05	0.63	7.64
[Co^{I}Cor]$^{[a]}$	0.42	−0.42	−1.98	–	7.74
[Fe^{II}Por]	0.66	−0.66	−2.41	2.04	6.47
[Fe^{II}Cor]$^+$	0.74	0.26	−2.16	2.09	6.49
[Co^{II}Por]	0.64	−0.64	−2.33	1.10	7.49
[Co^{II}Cor]$^+$	0.68	0.32	−2.09	1.10	7.50

[a] Closed-shell singlet state.

Reduction potential

Another possible reason for the selection of certain combinations of ions and rings is differences in the reduction potential between the two metal ions and the two ring systems. In aqueous solution, iron is more easily oxidised than cobalt. For example, the Co$^{0/II}$ potential (-0.28 V) is less negative than the corresponding Fe$^{0/II}$ potential (-0.44 V). Similarly, the Co$^{II/III}$ potential ($+1.82$ V) is more positive than the Fe$^{II/III}$ potential

(+0.77 V; all potentials are relative to the standard hydrogen electrode).[48] Therefore, we have studied the reduction potentials of the various complexes in the present investigation.

When calculating reduction potentials, solvation energies are as important as the electronic energies. These have been estimated by the COSMO continuum model, with three different values of the dielectric constant (ε): 1 (vacuum), 4, and 80. The last value is close to what is found in bulk water solution, whereas the whole series gives an impression of what effects can be expected inside a protein, where the effective dielectric constant has been estimated to be 2–16.[53, 54] The results of these calculations for the Im$_2$ and Im/Me complexes in their low-spin ground states are shown in Table 10.

Two clear trends can be seen from these results. First, a cobalt complex has a reduction potential that is 0.2–0.5 V *lower* than the corresponding iron complex. This represents the intrinsic difference between iron and cobalt with these ligands. The sign of the difference is somewhat unexpected, because it indicates that Co^{2+} is more easily oxidised than Fe^{2+} although the contrary is found for the ions in aqueous solution.[48] However, this is an effect of the tetrapyrrole rings; for the isolated and hydrated ions, similar calculations indicate that iron is the most easily oxidised ion (for example, the [M(H$_2$O)$_6$] complexes studied with $\varepsilon = 80$ reproduce exactly the experimental 0.99 V difference between Co$^{II/III}$ and Fe$^{II/III}$).[48] Thus, the ring systems selectively stabilise the Co^{III} state relative to the Fe^{III} species.

Second, it can be seen that porphine gives rise to a lower reduction potential than corrin does. The reason for this is that the double negative charge of the porphine ring stabilises (solvates) the higher charge of the oxidised state better than the single negative charge of corrin. The same argument also explains why the Im/Me complexes have lower reduction potentials than the Im$_2$ complexes.

We also see that the difference in reduction potential between porphine and corrin depends strongly on ε, but not so much on the metal. The reason for this is also the differing charge of the two ring systems, which leads to different total charges of the complexes. The solvation energy depends strongly on the total charge of the complex (compare with the simple Born model, in which the solvation energy is proportional to the square of the total charge). This explains why the reduction potential of all the complexes decreases with ε (the total charge increases during oxidation) except for the [MPorImMe] complexes, in which the total charge decreases during oxidation.

Together, the result of these two effects is that the two native combination species FePor and CoCor have quite similar reduction potentials (especially in water). The two other species have either higher (CoPor) or lower (FeCor) potentials, but the difference is not very large in water (0.2–0.5 V).

The reduction potential of the [FePorIm$_2$] complex ranges from −0.7 in water to +0.4 V in vacuum. This is in reasonable accordance with the measured reduction potentials of cytochromes, which range between −0.4 and +0.5 V.[5, 49] The corresponding [CoCorIm$_2$] model has a potential that is more sensitive to ε and is in general somewhat higher (−0.7 to +3.2 V). Thus, the reduction potentials give no clear reason why cobalt or corrin are not employed for biological electron transfer. Likewise, for the Im/Me complexes, the reduction potentials of [CoCorMeIm] and [FePorMeIm] partly overlap, although that of the former complex is in general higher.

An important reason for using corrin for heterolytic Co–C bond cleavage may be to make the the Co^{I} state accessible; this state would be anticipated to be unfavourable in a porphyrin ring, compared with species of higher oxidation state, due to increased interelectron repulsion in the ligand field. Thus, it has been suggested that the Co^{I} state is not accessible in CoPor systems,[10] and it has also been observed that [FeCor] can be oxidised to Fe^{I}, but it cannot be methylated.[11] Therefore, we have also studied the reduction potentials of the four-coordinate M^{I} and M^{II} complexes without any axial ligands. These results are also included in Table 10.

Interestingly, the reduction potentials of the four-coordinate complexes are similar to those of the six-coordinate complexes. Cobalt gives rise to slightly lower reduction potentials than does iron (0–0.2 V), but the difference is smaller and reversed at the highest dielectric constant, and there are large effects of the ring system, especially at low values of ε. However, the reduction potential of [FePor] is always lower than that of [CoCor]. The difference is largest at low values of ε, but even in water solution, the difference is predicted to be 0.4 V. Thus, it should be appreciably harder to form [Fe^{I}Por] than [Co^{I}Cor]. The same applies to [CoPor], which is quite similar to [FePor]; this confirms the suggestion that the Co^{I} state is not accessible in [CoPor].[10] Yet, the [FeCor] complex is predicted to be more easily reduced than the native [CoCor] complex.

Reorganisation energies

We will now turn to some functional aspects of the various combinations of ions and ring systems. We have concentrated on one typical reaction for each of the two native combinations, that is, the Co–C bond dissociation reaction as a typical reaction for the CoCor species in coenzyme B$_{12}$, and electron transfer as a typical reaction for FePor species in the cytochromes, although

Table 10. *Calculated reduction potentials for the [MCor/PorIm$_2$], [MCor/PorImMe] and four-coordinate [MCor/Por] complexes.*

MPor/Cor					Axial ligands				
		Im$_2$			Im/Me			–	
	$\varepsilon = 1$	$\varepsilon = 4$	$\varepsilon = 80$	$\varepsilon = 1$	$\varepsilon = 4$	$\varepsilon = 80$	$\varepsilon = 1$	$\varepsilon = 4$	$\varepsilon = 80$
CoPor	0.08	−0.69	−1.03	−3.96	−2.84	−2.29	−3.78	−2.53	−1.84
FePor	0.39	−0.38	−0.72	−3.81	−2.65	−2.05	−3.54	−2.43	−1.87
CoCor	3.26	0.56	−0.72	−0.98	−1.82	−2.20	−0.31	−1.14	−1.48
FeCor	3.53	0.84	−0.42	−0.52	−1.32	−1.67	−0.19	−1.11	−1.52

we recognise that haem proteins have a number of other functions.

Electron transfer is a special reaction, in that its only effect is to move an electron from one site to another. According to the semiclassical Marcus theory,[50] the rate of electron transfer depends on three terms, the reduction potential (which we have already studied), the electronic coupling element (which is mainly a function of the distance between the donor and the acceptor sites), and the reorganisation energy (λ). The latter term measures how much the geometry of the donor and acceptor sites changes during the redox process. It is normally divided into two contributions, the inner- and outer-sphere reorganisation energy (λ_i and λ_o), depending on what atoms are relaxed. For a metal-containing protein, the inner-sphere reorganisation energy is associated with the structural change of the first coordination sphere, whereas the outer-sphere reorganisation energy involves structural changes of the remaining protein as well as the solvent.

We have calculated the inner-sphere reorganisation energy for the four combinations of ions and ring systems. It is calculated as the energy difference of the reduced complex at its optimum geometry and at the optimum geometry of the oxidised complex (λ_{red}) or vice versa (λ_{ox}).[51] For a self-exchange reaction, $\lambda_i = \lambda_{red} + \lambda_{ox}$. This approach has been successfully applied to several proteins,[52–55] in particular for cytochrome models with various sets of axial ligands.[37]

The reorganisation energies of the Im_2 complexes (models of several *b*- and *c*-type cytochromes) are shown in Table 11. They show that the two iron complexes give almost the same reorganisation energy (8 – 9 kJ mol^{-1}). Therefore, an iron corrin species would form an electron-transfer site equally as excellent as an iron porphyrin, but at higher potentials. It has been shown[37] that the LS state of the site is essential for the low reorganisation energy, but we have seen that corrin stabilises the LS of iron even better than porphyrin. Therefore, the reorganisation energies do not give any clue as to why nature has selected porphyrins rather than corrins in the cytochromes.

However, for the two cobalt complexes in Table 11, the reorganisation energies are very large (179 – 197 kJ mol^{-1}). The reason for these high values is the large change in the Co–N_{Im} distances (owing to the occupied d_{z^2} orbital for Co^{II}; see Table 5). The iron systems have similar axial bond lengths (within 4 pm) for both oxidation states, owing to the fact that the d_{z^2} and $d_{x^2-y^2}$ orbitals are empty in both oxidation states.

Table 11. Calculated inner-sphere reorganisation energies [kJ mol^{-1}] for the [MCor/PorIm$_2$] (DZpdf/6 – 31G basis set) and [MCor/PorImMe] (TZPP basis set) complexes.*

Complex	λ_{ox}	λ_{red}	λ
[FePorIm$_2$]	5	4	8
[FeCorIm$_2$]	5	4	9
[CoPorIm$_2$]	105	74	179
[CoCorIm$_2$]	114	82	197
[FePorImMe]	3	1	5
[FeCorImMe]	6	3	9
[CoPorImMe]	6	6	13
[CoCorImMe]	18	11	29

This gives a direct explanation of why cobalt (at least the Co$^{II/III}$ couple in octahedral geometry) has not been used for electron transfer. A reorganisation energy of 179 – 197 kJ mole^{-1} is much larger than what is obtained for native electron-transfer sites (4 – 40 kJ mol^{-1}[37]). We conclude that evolutionary design of tetrapyrrole electron transfer systems may involve either corrins or porphyrins, but not Co$^{II/III}$ species.

Bond dissociation energies

As a typical reaction for the CoCor species in coenzyme B_{12}, we will study the homolytic Co–C bond dissociation energy (BDE), that is, the energy of the reaction shown in Equation (2).

$$[M^{III}Cor/PorImMe] \rightarrow [M^{II}Cor/PorIm] + Me^{\bullet} \quad (2)$$

The experimental BDE of methylcobalamin is 155 ± 12 kJ mol^{-1}.[56, 57] The Co–C bond strengths of various cobalamin models have been calculated with B3LYP density functional calculations by three groups.[24, 41, 42] They obtained BDE values of 91 – 117 kJ mole^{-1} when using the same type of model as we used ([CoCorImMe]), that is, far from the experimental value. Recently, we have shown that this is a shortcoming of the B3LYP method.[47] Other density functional calculations (for example, BP86) and second-order Møller – Plesset perturbation theory (MP2) give results close to the experimental value (148 – 160 kJ mol^{-1}). Therefore, we have calculated the Co–C BDE at the BP86 level of theory in this paper.

The calculated Co–C BDE values for the four combinations of ions and ligands are shown in Table 12. They are obtained for the lowest spin state for all reactants, that is, the LS state for all cobalt complexes and for the six-coordinate iron complexes, but the IS state of the five-coordinate iron complexes (see Table 2). It can be seen that the BDE values are quite similar, varying from 147 kJ mol^{-1} for the FePor species to 159 kJ mol^{-1} for the CoCor model. Solvation effects are small (1 – 7 kJ mol^{-1}) and do not change the order between the various complexes, as can also be seen in Table 12.

Table 12. Co–C BDE values [kJ mol^{-1}] for the [MCor/PorImMe] complexes, calculated with the DZpdf/6 – 31G(d) basis set.

Complex	BDE $\varepsilon = 1$	 $\varepsilon = 4$	 $\varepsilon = 80$
[FePorImMe]	146.7	144.2	142.7
[FeCorImMe]	148.0	147.5	147.6
[CoPorImMe]	156.4	153.4	151.5
[CoCorImMe]	158.6	157.7	157.5

Thus, the combination employed in nature has the *highest* Co–C BDE. This may at first seem a bit strange, because the Co–C bond is broken during the biochemical reaction. However, as Pratt has argued, the Co–C bond must be stable against hydrolysis.[11] In fact, he attributes the strong Co–C bond to the low 3d to 4s/4p promotion energy of Co^{II}, which gives strong covalent bonds with carbon.[11]

This has led us to study the hydrolysis of the six-coordinate Im/Me complexes, that is, the reaction shown in Equation (3).[11]

$$[\mathrm{M^{III}Cor/PorImMe}] + \mathrm{H_2O} \rightarrow [\mathrm{M^{III}Cor/PorImOH}] + \mathrm{CH_4} \quad (3)$$

The calculated reaction energies for the four combinations of ions and ring systems (using the LS ground state for all metal complexes) are shown in Table 13. They indicate that all the methyl complexes are unstable towards hydrolysis by 71–122 kJ mol^{-1}. However, the cobalt complexes are much more stable (by 33–48 kJ mol^{-1}) than the corresponding iron complexes. This gives a strong reason why cobalt is selected, rather than iron, as a methyl donor or radical carrier.

Table 13. Hydrolysis energies [kJ mol^{-1}] [Eq. (3)] for the [MCor/PorImMe] complexes, calculated with the DZpdf/6–31G(d) basis set.

Complex	Energy		
	$\varepsilon=1$	$\varepsilon=4$	$\varepsilon=80$
[FePorImMe]	−121.2	−117.8	−117.6
[FeCorImMe]	−122.2	−115.3	−112.4
[CoPorImMe]	−72.7	−75.4	−78.9
[CoCorImMe]	−75.5	−71.8	−70.7

Methyl-transfer reactions

Our results also give us the opportunity to study the other type of cobalamin reaction, that is, the heterolytic cleavage of the Co^{III}–C bond, giving a four-coordinate Co^{I} complex and formally a $\mathrm{CH_3^+}$ cation, which is transferred to a nucleophilic substrate, for example, homocysteine. This reaction can either be studied as a heterolytic Co–C bond dissociation as in [Eq. (4)] or with a substrate included, for example, $\mathrm{CH_3S^-}$ (as a model of homocysteine in a methionine-synthetase-like reaction) as shown in [Eq. (5)].

$$[\mathrm{M^{III}Cor/PorImMe}]^{+/0} \rightarrow [\mathrm{M^{I}Cor/Por}]^{0/-} + \mathrm{Im} + \mathrm{Me^+} \quad (4)$$

$$[\mathrm{M^{III}Cor/PorImMe}]^{+/0} + \mathrm{CH_3S^-} \rightarrow [\mathrm{M^{I}Cor/Por}]^{0/-} + \mathrm{Im} + \mathrm{CH_3SCH_3} \quad (5)$$

Both reactions give the same relative result, although the absolute values are shifted by a large constant. The results for the reaction in [Eq. (5)] are gathered in Table 14.

It can be seen that the reaction energy varies a great deal with the dielectric constant, as can be expected for a reaction altering the charges of the reactants. At a low dielectric constant, the corrin complexes give the most negative reaction energies, whereas in water solution, all four complexes are predicted to give similar reaction energies (within 12 kJ mol^{-1}). Therefore, the homolytic methyl-transfer reaction does not provide any clear explanation why the cobalamins were selected in nature. On the contrary, iron gives a 8–19 kJ mol^{-1} lower reaction energy than cobalt.

Table 14. Methyl-transfer energies [kJ mol^{-1}] [Eq. (5)] for the [MCor/PorImMe] complexes, calculated with the DZpdf/6–31G(d) basis set.

Complex	Energy		
	$\varepsilon=1$	$\varepsilon=4$	$\varepsilon=80$
[FePorImMe]	−149.4	−74.8	−135.2
[FeCorImMe]	−436.0	−176.0	−147.4
[CoPorImMe]	−127.6	−96.6	−145.2
[CoCorImMe]	−416.9	−163.0	−139.4

Concluding Remarks

In this paper, we have studied how the properties of iron and cobalt porphyrins and corrins differ in various aspects. The results have given us several clues as to how the seemingly similar structures of iron porphyrin and cobalt corrin give rise to their different functions.

First, we have seen that the thermodynamic stability favours the two native combinations of ions and ring systems by 8–24 kJ mol^{-1} over the nonnative combinations for all complexes, except the M^{II} with Im/Me complexes. Thus, there is some intrinsic thermodynamic reason to choose the native combinations.

Second, and probably most importantly, the central cavity of the corrin ring is smaller than that of the porphine ring. Therefore, corrin favours the low-spin states of Co^{III} and Co^{II}, and even the four-coordinate low-spin Co^{I} (formally) ion fits well into the corrin ring. Thus, CoCor species are always low spin and all reactants and intermediates in the cobalamin reaction cycles involve small strain in the ring system. On the other hand, the cavity in porphine is too large for the low-spin cobalt and iron ions. Instead, it seems to be more appropriate for the intermediate-spin states. Consequently, intermediate- and high-spin states are available for the FePor species, and they are important for many of the reactions of haem proteins, for example, in the binding and activation of $\mathrm{O_2}$.

Third, Co^{III} in aqueous solution is more easily reduced than iron. However, in the tetrapyrrole rings, this tendency has been reversed, so that cobalt consistently gives potentials that are 0.1–0.3 eV lower than those for iron. There are also pronounced differences in the reduction potentials of the corrin and porphine rings, in that the former gives higher potentials. These are mainly caused by the differing charge of the ring system and therefore strongly depend on solvation effects. As an effect of these two opposing tendencies, the native FePor and CoCor combinations often give quite similar reduction potentials at high dielectric constants, but the latter has a higher potential in most solvents. In particular, four-coordinate [Co^{I}Cor] is more easily formed than [Fe^{I}Por]; this means that it is accessible in corrin chemistry.

Fourth, the octahedral [Fe$^{II/III}$Por/CorIm$_2$] complexes have much lower inner-sphere reorganisation energies (8–9 kJ mol^{-1}) than the corresponding Co$^{II/III}$ complexes (179–197 kJ mol^{-1}). The reason for this is the occupation of the d_{z^2} orbital in low-spin Co^{II} (d^7), which leads to a large difference in the distances to the axial ligands in the two oxidation states. Therefore, the Co$^{II/III}$ couple is useless for electron-transfer reactions, whereas the octahedral Fe$^{II/III}$ complexes ($d^{5/6}$) form excellent electron carriers, also in comparison to other metal sites.[37]

Finally, [CoCorImMe] has the largest homolytic Co–C BDE of the studied complexes, even if the variation is only 12 kJ mol^{-1}. This is compensated by the largest resistance towards hydrolysis. The cobalt complexes are appreciably more stable towards hydrolysis than the iron complexes (by ≈40 kJ mol^{-1}). This may explain why cobalamins are employed in nature for organometallic reactions.

In conclusion, we have identified several good reasons for why iron is associated with porphine in nature whereas cobalt is associated with corrin, and also for why FePor species are used for electron transfer and oxygen activation whereas CoCor species are involved in organometallic Co–C reactions (methyl transfer and radical formation).

Methods

Models: We have included the full porphine (Por) or corrin (Cor) ring systems in our models, because this is the basic entity of the coenzymes and loss of equatorial conjugation energy may have a drastic effect on the electron structure. All side chains on the rings have been replaced by hydrogen atoms in the models to allow for a comparison of the fundamental chemistry of the corrin and porphine rings. Earlier calibrations have shown that they have a small influence on the structure and properties of the ring system.[58] We have studied five types of models that differ in their axial ligands: Three are octahedral with two axial ligands, either two imidazole groups (Im_2), one Im and one methyl group (Me) or one Im and one hydroxide ion. In addition, we studied five-coordinate complexes with an Im ligand and four-coordinate complexes without any axial ligands. The following oxidation states have been studied: M^{II} and M^{III} (M denotes the metal, Co or Fe) for the complexes with Im_2 and Im/Me, M^{III} for the Im/OH complexes, M^{II} for the five-coordinate complexes and M^{I} and M^{II} for the four-coordinate complexes. All systems were optimised in the lowest (ground) spin state, according to experiments or calculations. For the Im/Me, Im, and four-coordinate complexes, we also optimised the high- and intermediate-spin states. Some of the native combinations of ions and ring systems ([$Fe^{II/III}PorIm_2$], [$Co^{III}CorImMe$], [$Fe^{II/III}PorIm$], [$Co^{II}CorIm$], [$Fe^{II}Por$], [$Co^{II}Por$], [$Co^{I}Cor$]) have been studied before by theoretical methods,[16, 24–42] but only for the latter three has the aim been to compare the properties of the ions and rings.[16]

Computational Details: All calculations were performed with the Becke three-parameter hybrid functional method B3LYP, which combines some exact Hartree–Fock exchange with the local spin-density correlation functional of Vosko–Wilk–Nusair and the non-local Lee–Yang–Parr correlation functionals.[59] B3LYP is widely recognised as one of the most accurate density functional methods, in general terms, for structures, energies and frequencies.[60, 61] However, for the Co–C bond dissociation energy, calibration calculations have shown that B3LYP gives very poor results.[62] Therefore, we used the density functional Becke–Perdew 86 (BP86) method for these (single-point) energies.[63, 64]

The calculations were carried out with the TURBOMOLE program, versions 5.3 and 5.5.[65] The geometry optimisations were run with the 6–31G* basis set for all atoms except the metal. This basis set assigns one set of polarisation functions to all non-hydrogen atoms. For cobalt and iron, we used the double-ζ basis set of Schäfer et al. (contraction scheme 14s11p6d1f/8s7p4d1f),[66] augmented with two p, one d and one f functions (with exponents 0.141308, 0.043402, 0.1357 and 1.62 for Co and 0.134915, 0.41843, 0.1244 and 1.339 for Fe). Only the pure five d- and seven f-type functions were used. We applied the default (m3) grid size of TURBOMOLE, and all optimisations were carried out in redundant internal coordinates. Fully unrestricted calculations were performed for the open-shell systems. We made use of the default convergence criteria, which imply self-consistency down to 10^{-6} Hartree (2.6 J mol^{-1}) for the energy and 10^{-3} a.u. (0.053 pm or 0.057°) for the internal degrees of freedom.

After optimisation, accurate energies for most of the structures were calculated with the large triple-ζ 6–311+G(2d,2p) basis set, which includes diffuse functions on heavy atoms and polarisation functions on all atoms. The basis sets of the metals were augmented by one s function (with exponents 0.0145941 for Co and 0.01377232 for Fe) and the f function was replaced by two new functions (with exponents 2.8 and 0.8 for Co and 2.5 and 0.8 for Fe).

Solvation energies: Normal quantum chemical calculations are performed in vacuum, whereas most reactions take place in water solution or in proteins. In order to correct for this discrepancy, we have calculated solvation energies for most complexes with the continuum conductor-like screening model (COSMO),[67] as implemented in TURBOMOLE version 5.5. In this method, the solute molecule forms a cavity within a dielectric continuum characterised by a dielectric constant, ε. The charge distribution of the solute polarises the dielectric medium and the response of the medium is described by the generation of screening charges on the surface of the cavity.

These calculations were performed with default values for all parameters (implying a water-like probe molecule) and dielectric constants of 4 and 80, to model pure water and to get a feeling of possible effects in a protein (where the effective dielectric constant is normally estimated at 2–16).[68, 69] For the generation of the cavity, a set of atomic radii have to be defined. We used the optimised COSMO radii in TURBOMOLE (H: 1.30, C: 2.00, N: 1.83, O: 1.72, Fe: 2.00, Co: 2.00 Å).

Reduction potentials were estimated from these energies in a solvent according to [Eq. (6)], where the factor of 4.43 eV represents the potential of the standard hydrogen electrode.[70]

$$E^0 = E(\mathrm{ox}) - E(\mathrm{red}) - 4.43 \qquad (6)$$

This investigation has been supported by grants from the Swedish research council (VR) and by computer resources of Lunarc at Lund University.

[1] M. Sono, M. R. Roach, E. D. Coulter, J. H. Dawson, *Chem. Rev.* **1996**, *96*, 2841.

[2] J. P. Glusker, *Vitam. Horm.* **1995**, *50*, 1.

[3] M. L. Ludwig, R. G. Matthews, *Annu. Rev. Biochem.* **1997**, *66*, 269.

[4] R. Banerjee, *Chem. Biol.* **1997**, *4*, 175.

[5] J. J. R. Frausto da Silva, R. J. P. Williams, *The Biological Chemistry of the Elements*, Clarendon Press, Oxford, **1994**, p. 10.

[6] M. D. Wirt, I. Sagi, E. Chen, S. M. Frisbie, R. Lee, M. R. Chance, *J. Am. Chem. Soc.* **1991**, *113*, 5299.

[7] W. R. Scheidt, C. A. Reed, *Chem. Rev.* **1981**, *81*, 543.

[8] R. K. Suko, L. Poppe, J. Rétey, R. G. Finke, *Bioorg. Chem.* **1999**, *27*, 451.

[9] M. D. Wirt, I. Sagi, M. R. Chance, *Biophys. J.* **1992**, *63*, 412.

[10] W. Kaim, B. Schwederski, *Bioinorganic Chemistry: Inorganic Elements in the Chemistry of Life*, John Wiley & Sons, Chichester, **1994**, p. 42.

[11] J. M. Pratt, *Pure Appl. Chem.* **1993**, *65*, 1513.

[12] A. M. Stolzenberg, M. T. Stershic, *J. Am. Chem. Soc.* **1988**, *110*, 6391.

[13] J. J. R. Frausto da Silva, R. J. P. Williams, *The Biological Chemistry of the Elements*, Clarendon Press, Oxford, **1994**, p. 403.

[14] M. K. Geno, J. Halpern, *J. Am. Chem. Soc.* **1987**, *109*, 1238.
[15] S. J. Lippard, J. M. Berg, *Principles of Bioinorganic Chemistry*, University Science Books, Mill Valley, CA, **1994**, p. 343.
[16] C. Rovira, K. Kunc, J. Hutter, M. Parrinello, *Inorg. Chem.* **2001**, *40*, 11.
[17] R. J. P. Williams, *J. Mol. Catal.* **1985**, *30*, 1.
[18] Y. Murakami, Y. Aoyama, K. Tokunaga, *J. Am. Chem. Soc.* **1980**, *102*, 6736.
[19] J. M. Pratt in B_{12}, *Volumes 1 and 2*, (Ed.: D. Dolphin), Wiley, New York, **1982**, p. 325.
[20] E. Scheuring, R. Padmakumar, R. Banerjee, M. R. Chance, *J. Am. Chem. Soc.* **1997**, *119*, 12 192.
[21] S. Dong, R. Padmakumar, R. Banerjee, T. G. Spiro, *J. Am. Chem. Soc.* **1996**, *118*, 9182.
[22] S. Dong, R. Padmakumar, R. Banerjee, T. G. Spiro, *J. Am. Chem. Soc.* **1999**, *121*, 7063.
[23] J. M. Sirovatka, A. K. Rappé, R. G. Finke, *Inorg. Chim. Acta* **2000**, *300–302*, 545.
[24] K. P. Jensen, U. Ryde, *THEOCHEM* **2002**, *585*, 239.
[25] M.-M. Rohmer, *Chem. Phys. Lett.* **1985**, *116*, 44.
[26] W. D. Edwards, B. Weiner, M. C. Zerner, *J. Am. Chem. Soc.* **1986**, *108*, 2196.
[27] Y.-K. Choe, T. Hashimoto, H. Nakano, K. Hirao, *Chem. Phys. Lett.* **1998**, *295*, 380.
[28] Y.-K. Choe, T. Nakajima, K. Hirao, R. Lindh, *J. Chem. Phys.* **1999**, *111*, 3837.
[29] T. G. Spiro, P. M. Kozlowski, M. Z. Zgierski, *J. Raman Spectrosc.* **1998**, *29*, 869.
[30] P. M. Kozlowski, T. G. Spiro, A. Bérces, M. Z. Zgierski, *J. Phys. Chem. B* **1998**, *102*, 2603.
[31] Y. Seno, N. Kameda, J. Otsuka, *J. Chem. Phys.* **1980**, *72*, 6048.
[32] S. Obara, H. Kashiwagi, *J. Chem. Phys.* **1982**, *77*, 3155.
[33] S. Yamamoto, J. Teraoka, H. Kashiwagi, *J. Chem. Phys.* **1988**, *88*, 303.
[34] N. Matsuzawa, M. Ata, D. A. Dixon, *J. Phys. Chem.* **1995**, *99*, 7698.
[35] C. Rovira, K. Kunc, J. Hutter, P. Ballone, M. Parinello, *J. Phys. Chem. A* **1997**, *101*, 8914.
[36] E. Sigfridsson, U. Ryde, *J. Biol. Inorg. Chem.* **1999**, *4*, 99.
[37] E. Sigfridsson, M. H. M. Olsson, U. Ryde, *J. Phys. Chem. B* **2001**, *105*, 5546.
[38] T. Andruniow, M. Z. Zgierski, P. M. Kozlowski, *J. Phys. Chem. B* **2000**, *104*, 10 921.
[39] T. Andruniow, M. Z. Zgierski, P. M. Kozlowski, *Chem. Phys. Lett.* **2000**, *331*, 509.
[40] K. P. Jensen, S. P. A. Sauer, T. Liljefors, P.-O. Norrby, *Organometallics* **2001**, *20*, 550.
[41] N. Dölker, F. Maseras, A. Lledos, *J. Phys. Chem. B* **2001**, *105*, 7564.
[42] T. Andruniow, M. Z. Zgierski, P. M. Kozlowski, *J. Am. Chem. Soc.* **2001**, *123*, 2679.
[43] M. L. Ludwig, R. G. Matthews, *Annu. Rev. Biochem.* **1997**, *66*, 269.
[44] R. H. Holm, P. Kennepohl, E. I. Solomon, *Chem. Rev.* **1996**, *96*, 2239.
[45] A. Eschenmoser, *Angew. Chem.* **1988**, *100*, 5; *Angew. Chem. Int. Ed.* **1988**, *27*, 5.
[46] T. S. Rush III, P. M. Kozlowski, C. A. Piffat, R. Kumble, M. Z. Zgierski, T. G. Spiro, *J. Phys. Chem. B* **2000**, *104*, 5020.
[47] J. L. Hoard, *Science* **1971**, *174*, 1295.
[48] J. G. Stark, H. G. Wallace, *Chemistry Data Book*, John Murray, London, **1982**.
[49] H.-X. Zhou, *J. Biol. Inorg. Chem.* **1997**, *2*, 109.
[50] R. A. Marcus, N. Sutin, *Biochim. Biophys. Acta* **1985**, *811*, 265.
[51] A. Klimkans, S. Larsson, *Chem. Phys. Lett.* **1994**, *189*, 25.
[52] M. H. M. Olsson, U. Ryde, B. O. Roos, *Protein Sci.* **1998**, *7*, 2659.
[53] U. Ryde, M. H. M. Olsson, *Int. J. Quantum Chem.* **2001**, *81*, 335.
[54] E. Sigfridsson, M. H. M. Olsson, U. Ryde, *Inorg. Chem.* **2001**, *40*, 2509.
[55] M. H. M. Olsson, U. Ryde, *J. Am. Chem. Soc.* **2001**, *123*, 7866.
[56] B. D. Martin, R. G. Finke, *J. Am. Chem. Soc.* **1990**, *112*, 2419.
[57] B. D. Martin, R. G. Finke, *J. Am. Chem. Soc.* **1992**, *114*, 585.
[58] E. Sigfridsson, U. Ryde, *J. Biol. Inorg. Chem.* **2003**, *8*, 273.
[59] R. H. Hertwig, W. Koch, *Chem. Phys. Lett.* **1997**, *268*, 345.
[60] C. W. Bauschlicher, *Chem. Phys. Lett.* **1995**, *246*, 40.
[61] P. E. M. Siegbahn, M. R. A. Blomberg, *Chem. Rev.* **2000**, *100*, 421.
[62] K. P. Jensen, U. Ryde, *J. Phys. Chem. B* **2003**, submitted.
[63] A. D. Becke, *Phys. Rev. A* **1988**, *38*, 3089.
[64] J. P. Perdew, *Phys. Rev. B* **1986**, *33*, 8822.
[65] R. Alrichs, M. Bär, M. Häser, H. Horn, C. Kölmel, *Chem. Phys. Lett.* **1989**, *162*, 165.
[66] A. Schäfer, H. Horn, R. Ahlrichs, *J. Chem. Phys.* **1992**, *97*, 2571.
[67] A. Klamt, J. Schüürmann, *J. Chem. Soc. Perkin Trans. 2* **1993**, 799.
[68] K. A. Sharp, *Annu. Rev. Biophys. Biophys. Chem.* **1990**, *19*, 301.
[69] B. Honig, *Science* **1995**, *268*, 1144.
[70] H. Reiss, A. Heller, *J. Phys. Chem.* **1985**, *89*, 4207.

Received: July 3, 2002
Revised version: February 2, 2003 [F 449]